



Targeted molecular profiling uncovers true ceruminous adenomas with *HMGA2::WIF1* and ceruminous syringocystadenoma papilliferum with *BRAF* V600E

Lisa M. Rooper¹ · Lester D. R. Thompson² · Ankur R. Sangoi³ · Dwight Oliver⁴ · Jeffrey Gagan⁴ · Justin A. Bishop⁴

Received: 6 March 2025 / Revised: 20 August 2025 / Accepted: 27 August 2025

© The Author(s), under exclusive licence to Springer-Verlag GmbH Germany, part of Springer Nature 2025

Abstract

Ceruminous adenomas are benign neoplasms that arise from ceruminous glands in the external auditory canal. While these tumors are currently regarded as a single entity, they are divided into three histologically diverse subtypes: ceruminous syringocystadenoma papilliferum, ceruminous pleomorphic adenoma, and ceruminous adenoma not otherwise specified (NOS). Given the similarities of two of these subtypes to other tumors that occur at multiple anatomic sites, it is currently unclear whether ceruminous adenomas are truly a unified group. In this study, we performed targeted molecular profiling of 11 cases of ceruminous adenoma to clarify their classification. We identified *BRAF* V600E mutations (via PCR and/or immunohistochemistry) in five ceruminous syringocystadenomas papilliferum. We also identified *HMGA2::WIF1* fusions (via RNA sequencing) in five ceruminous adenomas NOS and one ceruminous pleomorphic adenoma. Tumors with *HMGA2::WIF1* fusion did not display the canalicular adenoma-like morphology seen in salivary gland pleomorphic adenomas with this fusion. Overall, these findings suggest that the three subtypes of ceruminous adenoma represent two biologically distinct groups. Recurrent *BRAF* V600E mutations in ceruminous syringocystadenoma papilliferum are parallel to those in cutaneous syringocystadenoma papilliferum. Histologic and molecular concordance suggests that ceruminous syringocystadenoma papilliferum should be part of the broader syringocystadenoma papilliferum category rather than a subtype of ceruminous adenoma. Conversely, *HMGA2::WIF1* fusions in ceruminous adenoma NOS and ceruminous pleomorphic adenoma suggest that a stromal component may not be an essential point of distinction between these groups. These residual true ceruminous adenomas all likely represent a specialized form of mixed tumor unique to the external ear.

Keywords Ear neoplasms · Ceruminous adenoma · Syringocystadenoma papilliferum · Pleomorphic adenoma · *BRAF* · *HMGA2::WIF1* · Immunohistochemistry · Molecular diagnostics

Introduction

The ceruminous glands are specialized apocrine glands that reside in the outer third to half of the external auditory canal and rarely give rise to neoplasms. Historically, the classification of such tumors was confused by highly variable terminology, with the generic appellation ceruminoma frequently applied to both benign and malignant lesions at this site [1–8]. Over the last few decades, ceruminous adenoma has emerged as the consensus name for benign glandular tumors arising from the ceruminous glands [7, 9]. Despite this unified terminology, the ceruminous adenoma category is still diverse, with three distinctive histologic subtypes recognized by the 5th Edition World Health Organization (WHO) Classification of Head and Neck Tumours [10]. Ceruminous syringocystadenomas

✉ Lisa M. Rooper
rooper@jhmi.edu

¹ Department of Pathology, The Johns Hopkins University School of Medicine, 401 N. Broadway, Baltimore, MD, USA

² Head and Neck Pathology Consultations, Woodland Hills, CA, USA

³ Department of Pathology, Stanford University, Stanford, CA, USA

⁴ Department of Pathology, University of Texas Southwestern Medical Center, Dallas, TX, USA

papilliferum are histologically identical to cutaneous syringocystadenoma papilliferum of other anatomic sites. Likewise, ceruminous pleomorphic adenoma is defined by its resemblance to salivary gland pleomorphic adenoma, including a prominent chondromyxoid stromal component. Finally, ceruminous adenomas not otherwise specified (NOS) are biphasic neoplasms with a combination of tubular and papillary growth. While these groups are all part of the ceruminous adenoma entity, their marked diversity in histologic appearance and similarity to biologically distinct tumors that occur at multiple anatomic sites raises questions as to whether they should truly be regarded as a single unified category. In this study, we evaluated the genetic underpinnings of all subtypes of ceruminous adenoma to evaluate the validity of their current classification in the molecular era.

Methods

Inclusion criteria

With approval from the institutional review board, we identified 11 cases of ceruminous adenoma from the authors' surgical pathology archives and consultation files. We reviewed all available histologic sections for each case to confirm the classification as ceruminous syringocystadenoma papilliferum, ceruminous pleomorphic adenoma, and ceruminous adenoma NOS based on criteria in the 5th Edition WHO Classification of Head and Neck Tumours [10]. We also confirmed tumor location in the external auditory canal and obtained clinical and demographic information from submitted clinical history or the electronic medical record.

BRAF immunohistochemistry

Based on previous literature documenting *BRAF* mutations in syringocystadenoma papilliferum of other anatomic sites [11–13], we performed BRAF V600E immunohistochemistry on all cases classified as ceruminous syringocystadenoma papilliferum and those cases of ceruminous pleomorphic adenoma and ceruminous adenoma NOS that had sufficient tissue available using a mouse monoclonal antibody for BRAF V600E protein (clone VE1; 1:400 dilution; Abcam, Cambridge, MA). Stains were performed on Ventana BenchMark Ultra autostainers (Roche/Ventana Medical Systems, Tucson, AZ) using standardized automated protocols and appropriate positive and negative controls. The Ventana ultraView polymer detection kit was used to visualize signals. Tumors were regarded as positive on the basis of granular cytoplasmic staining in greater than 10% of cells.

BRAF PCR

We also performed *BRAF* mutation analysis via polymerase chain reaction (PCR)/mass spectrometry on all ceruminous syringocystadenoma papilliferum that had sufficient tissue available. Tumor DNA was extracted from microdissected deparaffinized tissue sections using the QIAamp DNA FFPE kit (Qiagen, Hilden, Germany) and assessed using Agena iPLEX chemistry (Agena Bioscience, San Diego, CA). All assay primers were designed using Agena MassARRAY Assay Design Suite software. *BRAF* exons 11 and 15 were PCR amplified and subsequently analyzed at hotspot codons, including valine 600, using single-base primer extension. Final products were analyzed by MALDI-TOF mass spectrometry on an Agena MassARRAY Analyzer 4, with *BRAF* genotyping calls made by manual inspection of spectrograms. The assay limit of detection is 10% mutant alleles.

RNA sequencing

Based on the extensive prevalence of gene fusions in salivary gland tumors and their analogues, we also performed RNA sequencing on all cases classified as ceruminous pleomorphic adenoma and ceruminous adenoma NOS as previously described [14]. In short, RNA was isolated using Qiagen AllPrep kits (Qiagen, Germantown, MD); custom NimbleGen probes (Roche, Indianapolis, IN) were used to create an enriched library containing all exons from 1505 cancer-related genes, and sequencing was performed on an Illumina NextSeq 550 (Illumina, San Diego, CA) with a median 900× target exon coverage. All fusions and variants were reviewed in the Integrated Genomics Viewer (Broad Institute, Cambridge, MA). The Star-Fusion algorithm was used to call fusions. The BRAF V600 locus was reviewed manually for BRAF *V600E* alterations.

HMG2 FISH

In light of the results of RNA sequencing, three cases of ceruminous syringocystadenoma papilliferum also underwent fluorescence in situ hybridization (FISH) for *HMG2* rearrangement. Formalin-fixed paraffin-embedded tissue sections were deparaffinized, pretreated with sodium thiocyanate (for 25 min at 80 °C), digested with protease (for 37 min at 37 °C), and dehydrated in alcohol. An HMG2 break part probe (12q14.3) (Empire Genomics, Depew, NY) was applied and sealed under cover glass. Probe and genomic DNA were co-denatured at 80 °C for 5 min, and hybridization was carried out overnight at 37 °C, followed by washing and staining with DAPI. Signal pattern in at

least 200 nuclei from each case was evaluated under a Zeiss fluorescent microscope.

Results

Clinical and demographic information

Results are summarized in Table 1. The eleven cases of ceruminous adenoma were taken from seven males and four females with a median age of 53 years (range 40–78 years). All tumors were located in the external auditory canal. These cases were subclassified as ceruminous syringocystadenoma papilliferum ($n=5$), ceruminous adenoma NOS ($n=5$), and ceruminous pleomorphic adenoma ($n=1$).

Ceruminous syringocystadenoma papilliferum

The five ceruminous syringocystadenomas papilliferum included both an endophytic glandular component and exophytic squamous surface (Fig. 1A). The glandular component was composed of tubules and papillae lined by a biphasic population of low columnar luminal cells surrounded by small cuboidal basal cells (Fig. 1B). They communicated with the overlying epidermis, transitioning to squamous-lined papillary projections with prominent surface hyperkeratosis. Ceroid granules were not identified within the cytoplasm of any cell population. The stroma had a dense population of plasma cells (Fig. 1C). Immunostains for mutant BRAF V600E protein were positive in all cases, with strong staining in the glandular component and weaker staining in the papillary projections (Fig. 1D). The three cases with sufficient tissue available for PCR also demonstrated BRAF V600E mutations.

Ceruminous adenoma NOS

The five ceruminous adenomas NOS were well-circumscribed but unencapsulated tumors with predominantly glandular architecture. Most cases showed a cellular population of small to medium-sized tubules with scattered early papillary excrescences (Fig. 2A). One case formed prominent large, simple cysts (Fig. 2B). Another case showed more complex papillary architecture projecting into a cystic space (Fig. 2C). The ceruminous adenoma NOS was uniformly composed of a biphasic population of cuboidal to columnar ductal cells with a moderate amount of eosinophilic cytoplasm and compact myoepithelial cells with scant amphophilic cytoplasm (Fig. 2D). The luminal cells had variable apocrine architecture, with areas that had more abundant eosinophilic cytoplasm, luminal snouting, and even rare apocrine-type cytologic atypia with vesicular chromatin and prominent nucleoli (Fig. 2E). No true pleomorphism, significant mitotic activity, or necrosis was seen. Most cases displayed dense yellow ceroid granules within apocrine cells (Fig. 2F). On RNA sequencing, all five ceruminous adenomas NOS harbored *HMGA2::WIF1* fusions. Breakpoints for all cases included *HMGA2* exon 3 and *WIF1* exon 10. The two cases that were evaluated were negative for BRAF V600E immunohistochemistry.

Ceruminous pleomorphic adenoma

The one ceruminous pleomorphic adenoma had areas that were identical to the ceruminous adenomas NOS, with well-circumscribed but unencapsulated borders and predominantly tubular architecture with focal papillary excrescences (Fig. 3A). However, it was notable for a well-developed chondromyxoid stromal component with overt cartilaginous differentiation (Fig. 3B). The tumor was largely composed of

Table 1 Clinical, immunohistochemical, and molecular findings

Case	Age	Sex	Subtype	BRAF V600E	HMGA2 fusion
1	40	F	Ceruminous syringocystadenoma papilliferum	Positive (PCR and IHC)	Negative (<i>HMGA2</i> FISH)
2	51	M	Ceruminous syringocystadenoma papilliferum	Positive (PCR and IHC)	NA
3	69	M	Ceruminous syringocystadenoma papilliferum	Positive (PCR and IHC)	NA
4	53	M	Ceruminous syringocystadenoma papilliferum	Positive (IHC)	Negative (<i>HMGA2</i> FISH)
5	45	M	Ceruminous syringocystadenoma papilliferum	Positive (IHC)	Negative (<i>HMGA2</i> FISH)
6	50	M	Ceruminous adenoma NOS	Negative (RNA-seq)	<i>HMGA2::WIF1</i> (RNA-seq)
7	68	F	Ceruminous adenoma NOS	Negative (RNA-seq)	<i>HMGA2::WIF1</i> (RNA-seq)
8	45	F	Ceruminous adenoma NOS	Negative (RNA-seq and IHC)	<i>HMGA2::WIF1</i> (RNA-seq)
9	58	M	Ceruminous adenoma NOS	Negative (RNA-seq)	<i>HMGA2::WIF1</i> (RNA-seq)
10	78	M	Ceruminous adenoma NOS	Negative (RNA-seq and IHC)	<i>HMGA2::WIF1</i> (RNA-seq)
11	71	F	Ceruminous pleomorphic adenoma	Negative (RNA-seq and IHC)	<i>HMGA2::WIF1</i> (RNA-seq)

FISH Fluorescence in situ hybridization, *IHC* Immunohistochemistry, *NA* not assessed, *NOS* not otherwise specified, *PCR* polymerase chain reaction, *RNA-seq* RNA sequencing

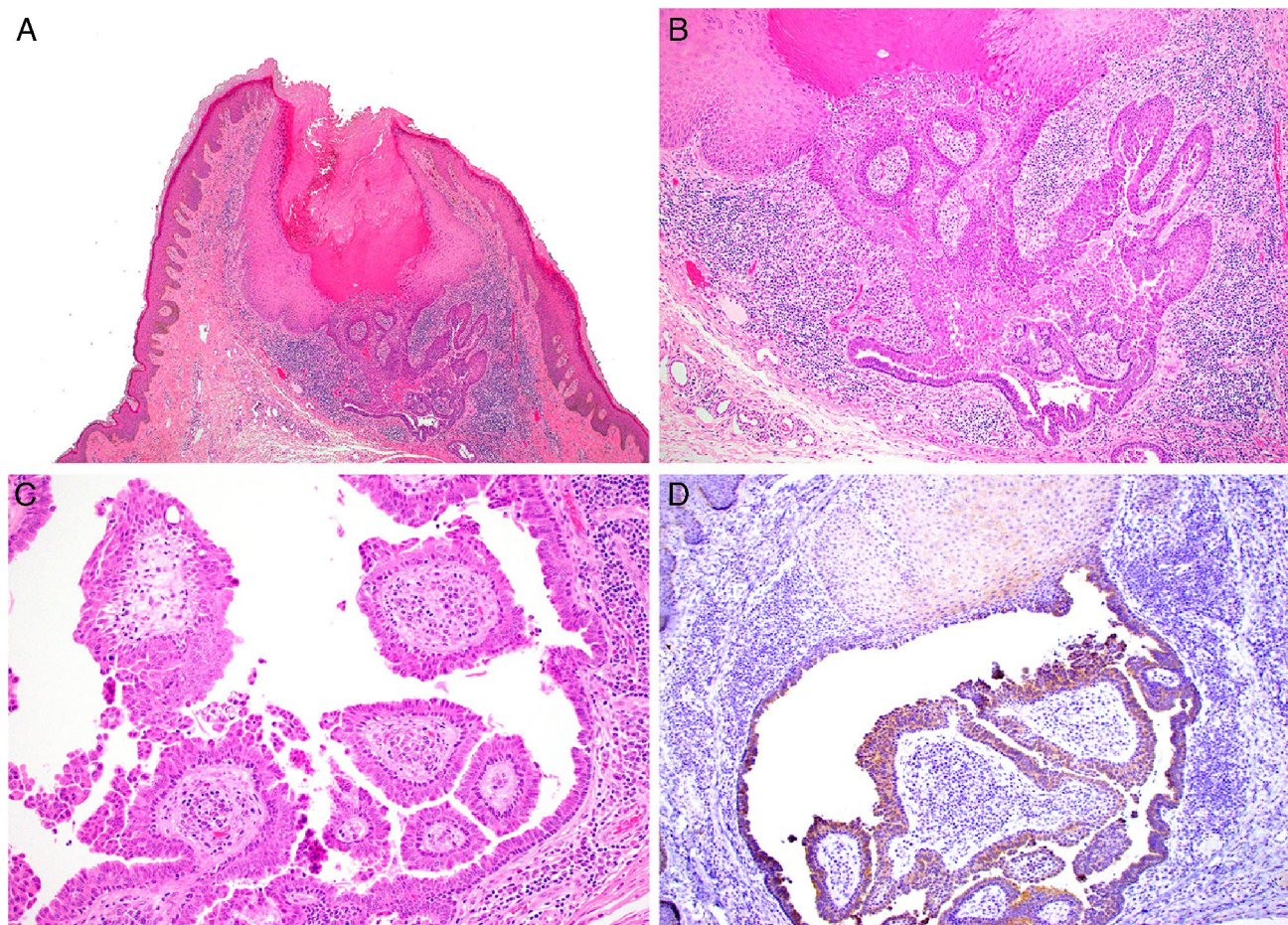


Fig. 1 Ceruminous syringocystadenomas papilliferum were composed of an endophytic glandular component and exophytic squamous component (**A**, 4×). The glandular component consisted of a biphasic population of low columnar luminal cells surrounded by small cuboidal basal cells arranged in tubules and papillae (**B**, 10×).

There was a dense population of plasma cells in the stroma (**C**, 20×). All ceruminous syringocystadenoma papilliferum were positive for mutant BRAF V600E immunohistochemistry, with strong staining in the glands and weaker staining in the squamous areas (**D**, 20×)

a biphasic population of plump eosinophilic ductal cells and more attenuated myoepithelial cells (Fig. 3C), although focal areas of more well-developed apocrine differentiation were seen (Fig. 3D). The ceruminous pleomorphic adenoma also harbored *HMGA2::WIF1* fusion with breakpoint at *HMGA2* exon 3 and *WIF1* exon 10. It was negative for BRAF V600E immunohistochemistry.

Discussion

Despite a historically variable classification, benign neoplasms of the ceruminous glands have been recognized under the unified term ceruminous adenoma for the last few decades [1–8]. However, this single categorization still belies a heterogeneous group of neoplasms that are divided into three histologic subtypes. Of these subtypes, ceruminous adenoma NOS is the only category that is not defined

based on its similarity to another tumor type. Given this histologic diversity and parallels with equally distinctive tumors from different anatomic sites, it is still not clear that ceruminous adenoma should be regarded as a single unified entity. In this study, we performed detailed histologic and molecular evaluation of all three subtypes of ceruminous adenoma to clarify its classification.

First, this study documents that ceruminous syringocystadenoma papilliferum harbors recurrent *BRAF* V600E mutations, reinforcing similarities with their cutaneous analogues. Ceruminous syringocystadenomas papilliferum are named for their histologic overlap with cutaneous syringocystadenoma papilliferum, with characteristic surface squamous papillations and underlying biphasic tubular proliferation. The five cases of ceruminous syringocystadenoma papilliferum in this series all demonstrated these classic features. *BRAF* V600E mutations are well-established as the molecular driver of cutaneous syringocystadenoma

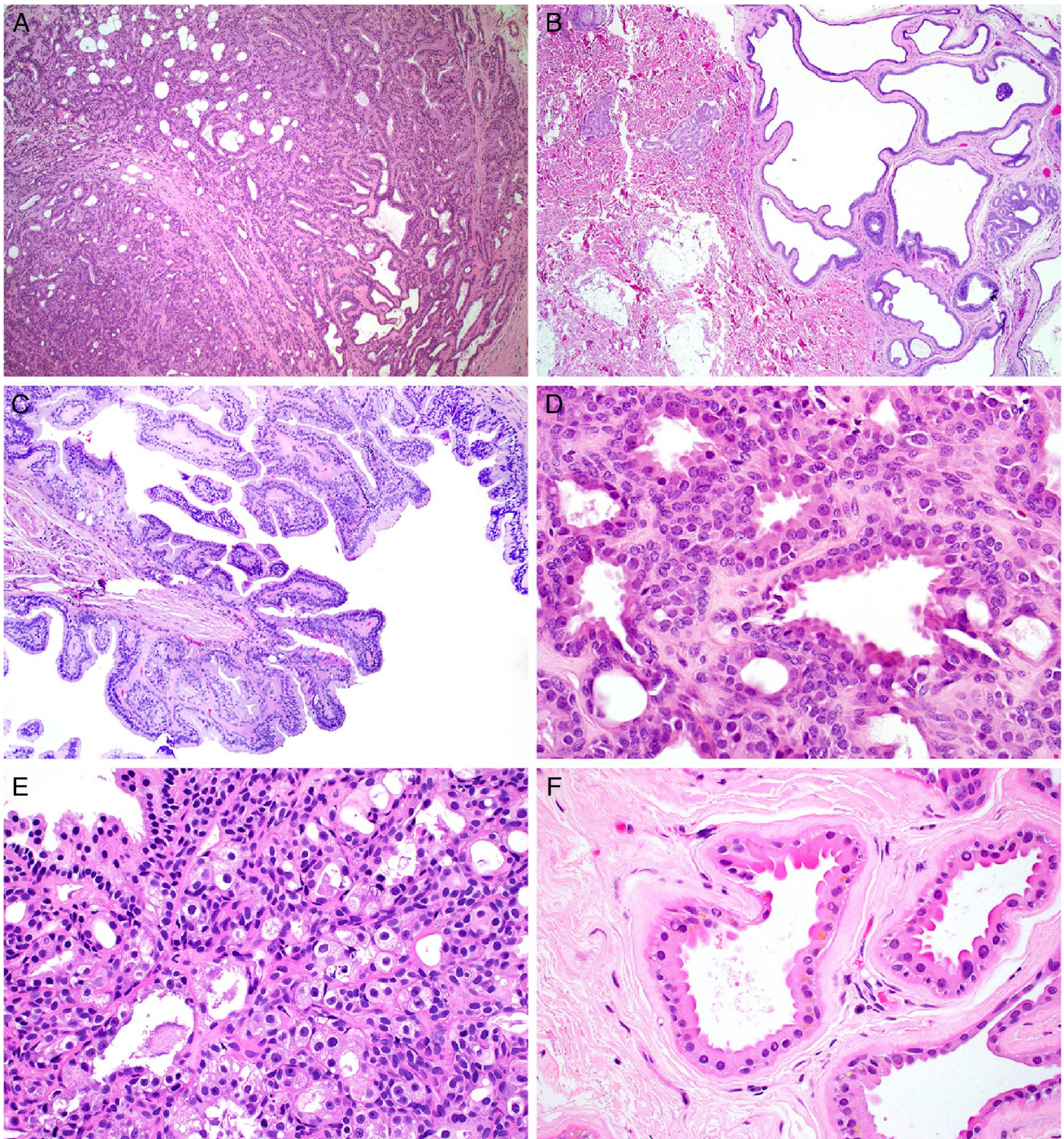


Fig. 2 Most ceruminous adenomas NOS were composed of small to medium-sized tubules with occasional early papillary excrescences (**A**, 4×), although one case formed large simple cysts (**B**, 4×) and another showed more complex papillary architecture (**C**, 10×). They contained a biphasic population of cuboidal to columnar ductal cells

with eosinophilic cytoplasm and compact myoepithelial cells with scant cytoplasm (**D**, 40×). The luminal cells had variable apocrine differentiation, including areas with luminal snouting, vesicular chromatin, and prominent nucleoli (**E**, 40×). Most ceruminous adenomas NOS had prominent yellow ceroid granules (**F**, 40×)

papilliferum at other anatomic sites [11–13]. Unsurprisingly, our results demonstrated that ceruminous syringocystadenoma papilliferum also has *BRAF* V600E mutations, with immunohistochemical expression of mutant *BRAF* V600E

protein in all five cases as well as molecular confirmation in all three cases tested by PCR. These findings indicate that cutaneous and ceruminous syringocystadenoma papilliferum are both morphologically and molecularly identical.

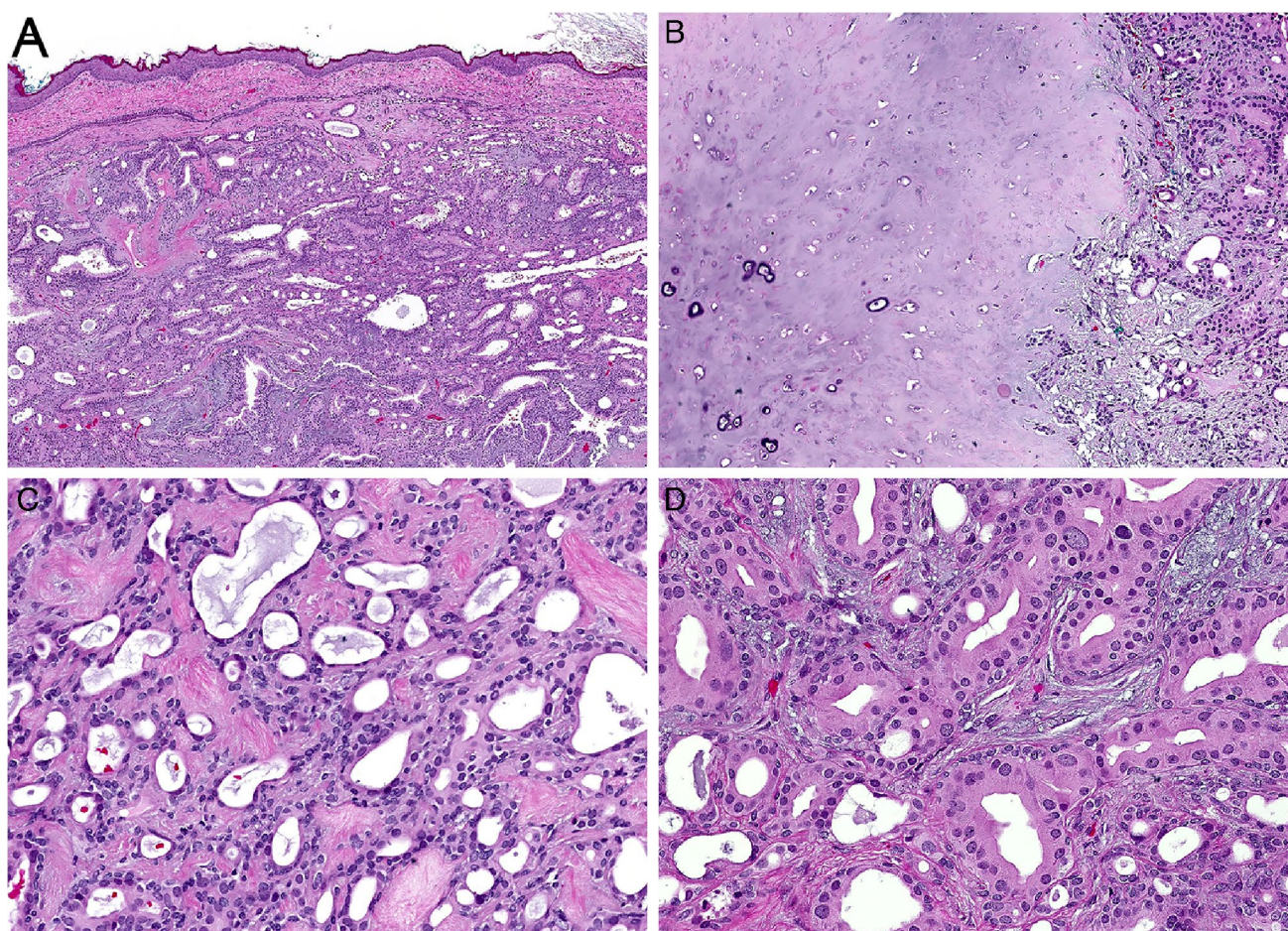


Fig. 3 The ceruminous pleomorphic adenoma demonstrated predominant tubular architecture with focal papillary excrescences that were identical to the ceruminous adenoma NOS (A, 4×). It also contained a prominent chondromyxoid stromal component (B, 10×). The tumor

cells were biphasic, including plump eosinophilic ductal cells and attenuated myoepithelial cells (C, 20×) with focal well-developed apocrine differentiation (D, 40×)

Of note, ceruminous syringocystadenoma papilliferum also has significant overlap with sialadenoma papilliferum of the salivary glands, which also harbors *BRAF* V600E mutations [15] and is the mucosal analogue to cutaneous syringocystadenoma papilliferum.

These findings also demonstrate that ceruminous adenoma NOS consistently harbors *HMGA2::WIF1* fusions, as does the single case of ceruminous pleomorphic adenoma tested. Ceruminous pleomorphic adenoma is named for its morphologic similarity to pleomorphic adenoma of the salivary glands. The presence of *HMGA2::WIF1* fusion in one case suggests that these similarities extend to the molecular level, as the majority of salivary pleomorphic adenomas harbor either *PLAG1* or *HMGA2* fusions with a variety of partners [16–20]. While ceruminous adenomas NOS also are composed of a biphasic population of ductal and myoepithelial cells that show some histologic overlap with pleomorphic adenoma, they have always been regarded as a separate subtype because they lack a significant stromal

component. However, in a limited sample, all cases of ceruminous adenoma NOS also have *HMGA2::WIF1* fusions. These identical molecular underpinnings suggest that ceruminous adenoma NOS may also be related to pleomorphic adenoma despite the absence of chondromyxoid stroma. Indeed, both ceruminous pleomorphic adenoma and ceruminous adenoma NOS may most closely overlap with mixed tumors of the skin—the cutaneous analogue to pleomorphic adenoma—which frequently have more scant fibrous or hyalinized stroma than their salivary counterparts and can also harbor *PLAG1* or *HMGA2* fusions [21, 22].

Interestingly, the ceruminous adenomas with *HMGA2::WIF1* fusions lack the distinctive morphology that has been reported in association with this fusion in salivary gland pleomorphic adenomas. Agaimy et al. recently described a large series of parotid gland tumors with prominent corded and trabecular growth that mimicked canalicular adenomas and had recurrent *HMGA2::WIF1* fusions [23]; this histo-molecular correlation has since been confirmed by

others [24–27]. Because a subset of these tumors shows more conventional pleomorphic adenoma morphology, including well-developed chondromyxoid stroma and variable architecture, these tumors, even without a stromal component, are currently regarded as part of the pleomorphic adenoma spectrum [23, 24]. Despite consistent *HMGA2::WIF1* fusions, ceruminous adenomas NOS and ceruminous pleomorphic adenomas lack this canalicular adenoma-like morphology in our cohort. This observation is likely a morphologic curiosity and does not carry any practical significance at this point, but is notable given this well-established molecular concordance.

Ultimately, these findings challenge the current classification of ceruminous adenomas as a single entity with three subtypes, suggesting instead that this traditional category is composed of two biologically distinct groups. Given their unique histologic and molecular features, the only attribute that binds ceruminous syringocystadenoma papilliferum together with ceruminous pleomorphic adenoma and ceruminous adenoma NOS is anatomic site. Instead, ceruminous syringocystadenoma papilliferum seems to fit better under the broader umbrella of cutaneous syringocystadenomas papilliferum, which are histologically identical and share common *BRAF* V600E mutations. Conversely, parallel *HMGA2::WIF1* fusions in ceruminous adenoma and ceruminous pleomorphic adenoma raise the possibility, albeit in a limited sample, that these subtypes are truly a single category, and a chondromyxoid stromal component may not be an essential point of distinction between these groups. While validation is needed in a larger cohort, both ceruminous pleomorphic adenoma and ceruminous adenoma NOS appear to represent a specialized subgroup of mixed tumor with apocrine and ceroid differentiation that is unique to the external auditory canal. As such, these external ear tumors with *HMGA2::WIF1* fusions may be best regarded as the true ceruminous adenomas.

Author contribution LR and JAB designed the study, performed data collection and interpretation, and prepared the manuscript. LDRT, ARS, DO, and JG performed data collection and interpretation. All authors read and approved the final paper.

Funding This study was funded by the Jane B. and Edwin P. Jenevein M.D. Endowment for Pathology at UT Southwestern Medical Center. No external funding was obtained for this study.

Data availability All data generated or analyzed during this study are included in this published article.

Declarations

Ethics approval All procedures performed in this retrospective data analysis involving human participants were in accordance with the ethical standards of the institutional review board (UT Southwestern IRB 112017–073).

Consent for publication The IRB-approved study did not require informed consent or consent for publication.

Conflict of interest The authors declare no competing interests.

References

1. Cankar V, Crowley H (1964) Tumors of ceruminous glands: a clinicopathologic study of 7 cases. *Cancer* 17:67–75. [https://doi.org/10.1002/1097-0142\(196401\)17:1%3c67::aid-cnrcr2820170109%3e3.0.co;2-a](https://doi.org/10.1002/1097-0142(196401)17:1%3c67::aid-cnrcr2820170109%3e3.0.co;2-a)
2. Dehner LP, Chen KT (1980) Primary tumors of the external and middle ear. Benign and malignant glandular neoplasms. *Arch Otolaryngol* 106(1):13–19. <https://doi.org/10.1001/archotol.1980.00790250015004>
3. Hicks GW (1983) Tumors arising from the glandular structures of the external auditory canal. *Laryngoscope* 93(3):326–340. <https://doi.org/10.1288/00005537-198303000-00016>
4. Lynde CW, McLean DI, Wood WS (1984) Tumors of ceruminous glands. *J Am Acad Dermatol* 11(5 Pt 1):841–847. [https://doi.org/10.1016/s0190-9622\(84\)80461-2](https://doi.org/10.1016/s0190-9622(84)80461-2)
5. Mansour P, George MK, Pahor AL (1992) Ceruminous gland tumours: a reappraisal. *J Laryngol Otol* 106(8):727–732. <https://doi.org/10.1017/s0022215100120717>
6. Mills RG, Douglas-Jones T, Williams RG (1995) ‘Ceruminoma’—a defunct diagnosis. *J Laryngol Otol* 109(3):180–188
7. Thompson LD, Nelson BL, Barnes EL (2004) Ceruminous adenomas: a clinicopathologic study of 41 cases with a review of the literature. *Am J Surg Pathol* 28(3):308–318. <https://doi.org/10.1097/00000478-200403000-00003>
8. Wetli CV, Pardo V, Millard M, Gerston K (1972) Tumors of ceruminous glands. *Cancer* 29(5):1169–1178. [https://doi.org/10.1002/1097-0142\(197205\)29:5%3c1169::aid-cnrcr2820290507%3e3.0.co;2-8](https://doi.org/10.1002/1097-0142(197205)29:5%3c1169::aid-cnrcr2820290507%3e3.0.co;2-8)
9. Nagarajan P (2018) Ceruminous neoplasms of the ear. *Head Neck Pathol* 12(3):350–361. <https://doi.org/10.1007/s12105-018-0909-3>
10. Sandison A, Thompson LDR (2022) Ceruminous adenoma. In: WHO Classification of Tumours Editorial Board (ed) WHO Classification of Head and Neck Tumours, 5th edn. International Agency for Research on Cancer, Lyon, France, pp 431–433
11. Konstantinova AM, Kyrpychova L, Nemcova J, Sedivcova M, Biscaglia M, Kutzner H et al (2019) Syringocystadenoma papilliferum of the anogenital area and buttocks: a report of 16 cases, including human papillomavirus analysis and HRAS and BRAF V600 mutation studies. *Am J Dermatopathol* 41(4):281–285. <https://doi.org/10.1097/DAD.0000000000001285>
12. Levinsohn JL, Sugarman JL, Bilguvar K, McNiff JM, Choate KA (2015) The Yale Center For Mendelian G. Somatic V600E BRAF mutation in linear and sporadic syringocystadenoma papilliferum. *J Invest Dermatol* 135(10):2536–2538. <https://doi.org/10.1038/jid.2015.180>
13. Shen AS, Peterhof E, Kind P, Rutten A, Zelger B, Landthaler M et al (2015) Activating mutations in the RAS/mitogen-activated protein kinase signaling pathway in sporadic trichoblastoma and syringocystadenoma papilliferum. *Hum Pathol* 46(2):272–276. <https://doi.org/10.1016/j.humpath.2014.11.002>
14. Bishop JA, Gagan J, Baumhoer D, McLean-Holden AL, Oliai BR, Couce M et al (2020) Sclerosing polycystic “adenosis” of salivary glands: a neoplasm characterized by PI3K pathway alterations more correctly named sclerosing polycystic adenoma. *Head Neck Pathol* 14(3):630–636. <https://doi.org/10.1007/s12105-019-01088-0>

15. Hsieh MS, Bishop JA, Wang YP, Poh CF, Cheng YL, Lee YH et al (2020) Salivary sialadenoma papilliferum consists of two morphologically, immunophenotypically, and genetically distinct subtypes. *Head Neck Pathol* 14(2):489–496. <https://doi.org/10.1007/s12105-019-01068-4>
16. Afshari MK, Tejera Nevado P, Fehr A, Huang J, Jawert F, Nilsson JA et al (2025) The transcriptomic and gene fusion landscape of pleomorphic salivary gland adenomas. *Genes Chromosomes Cancer* 64(1):e70023. <https://doi.org/10.1002/gcc.70023>
17. Andreasen S, von Holstein SL, Homoe P, Heegaard S (2018) Recurrent rearrangements of the PLAG1 and HMGA2 genes in lacrimal gland pleomorphic adenoma and carcinoma ex pleomorphic adenoma. *Acta Ophthalmol* 96(7):e768–e771. <https://doi.org/10.1111/aos.13667>
18. Asahina M, Saito T, Hayashi T, Fukumura Y, Mitani K, Yao T (2019) Clinicopathological effect of PLAG1 fusion genes in pleomorphic adenoma and carcinoma ex pleomorphic adenoma with special emphasis on histological features. *Histopathology* 74(3):514–525. <https://doi.org/10.1111/his.13759>
19. Kas K, Roijer E, Voz M, Meyen E, Stenman G, Van de Ven WJ (1997) A 2-Mb YAC contig and physical map covering the chromosome 8q12 breakpoint cluster region in pleomorphic adenomas of the salivary glands. *Genomics* 43(3):349–358. <https://doi.org/10.1006/geno.1997.4819>
20. Roijer E, Kas K, Behrendt M, Van de Ven W, Stenman G (1999) Fluorescence in situ hybridization mapping of breakpoints in pleomorphic adenomas with 8q12-13 abnormalities identifies a subgroup of tumors without PLAG1 involvement. *Genes Chromosomes Cancer* 24(1):78–82. [https://doi.org/10.1002/\(sici\)1098-2264\(199901\)24:1%3c78::aid-gcc11%3e3.0.co;2-d](https://doi.org/10.1002/(sici)1098-2264(199901)24:1%3c78::aid-gcc11%3e3.0.co;2-d)
21. Mansour B, Donati M, Pancsa T, Grossman P, Šteiner P, Vaněček T et al (2025) Molecular analysis of apocrine mixed tumors and cutaneous myoepitheliomas: a comparative study confirming a continuous spectrum of one entity with near-ubiquitous PLAG1 and rare mutually exclusive HMGA2 gene rearrangements. *Virchows Arch* 486(2):215–223. <https://doi.org/10.1007/s00428-024-03811-x>
22. Macagno N, Kervarrec T, Thanguturi S, Sohler P, Pissaloux D, Mescam L et al (2024) SOX10-internal tandem duplications and PLAG1 or HMGA2 fusions segregate eccrine-type and apocrine-type cutaneous mixed tumors. *Mod Pathol* 37(3):100430. <https://doi.org/10.1016/j.modpat.2024.100430>
23. Agaimy A, Ihrler S, Banekova M, Costes Martineau V, Mantopoulos K, Hartmann A et al (2022) HMGA2-WIF1 rearrangements characterize a distinctive subset of salivary pleomorphic adenomas with prominent trabecular (canalicular adenoma-like) morphology. *Am J Surg Pathol* 46(2):190–199. <https://doi.org/10.1097/PAS.0000000000001783>
24. Alsugair Z, Lepine C, Descotes F, Lanic MD, Pissaloux D, Tirode F et al (2024) Beneath HMGA2 alterations in pleomorphic adenomas: pathological, immunohistochemical, and molecular insights. *Hum Pathol* 152:105633. <https://doi.org/10.1016/j.humpath.2024.105633>
25. Brown AE, Eells AC, Hinni ML, Schmitt AC (2024) Canalicular-like pleomorphic adenoma of the parotid gland: a recently classified tumor highlighting the use of frozen section analysis and surrogate IHC for gene rearrangement defined subtypes. *Int J Surg Pathol* 32(8):1547–1551. <https://doi.org/10.1177/10668969241231980>
26. Dababneh MN, Azzato EM, Nakitandwe J, Cracolici V, Shah AA (2025) HMGA2-positive salivary gland neoplasms with prominent trabecular/canalicular morphology: a focus on carcinomas arising within this phenotype. *Histopathology* 86(3):385–396. <https://doi.org/10.1111/his.15334>
27. Katabi N, Sukhadia P, DiNapoli SE, Weinreb I, Hahn E, Ghossein R et al (2024) Expanding the histological spectrum of salivary gland neoplasms with HMGA2::WIF1 fusion emphasising their malignant potential: a report of eight cases. *Histopathology* 84(2):387–398. <https://doi.org/10.1111/his.15074>

Publisher's Note Springer Nature remains neutral with regard to jurisdictional claims in published maps and institutional affiliations.

Springer Nature or its licensor (e.g. a society or other partner) holds exclusive rights to this article under a publishing agreement with the author(s) or other rightsholder(s); author self-archiving of the accepted manuscript version of this article is solely governed by the terms of such publishing agreement and applicable law.